Biol Trace Elem Res (2013) 151:451–461
DOI 10.1007/s12011-012-9570-y

Divalent Heavy Metal Cations Block the TRPV1 Ca^{2+} Channel

László Pecze · Zoltán Winter · Katalin Jósvay · Ferenc Ötvös · Csongor Kolozsi · Csaba Vizler · Dénes Budai · Tamás Letoha · György Dombi · Gerda Szakonyi · Zoltán Oláh

Received: 4 May 2012 / Accepted: 3 December 2012 / Published online: 21 December 2012

Abstract Transient receptor potential vanilloid 1 (TRPV1) is a non-selective cation channel involved in pain sensation and in a wide range of non-pain-related physiological and pathological conditions. The aim of the present study was to explore the effects of selected heavy metal cations on the function of TRPV1. The cations ranked in the following sequence of pore-blocking activity: Co^{2+} [half-maximal inhibitory concentration (IC_{50})=13 μM]>Cd^{2+} (IC_{50}=38 μM)>Ni^{2+} (IC_{50}=62 μM)>Cu^{2+}(IC_{50}=200 μM). Zn^{2+} proved to be a weak (IC_{50}=27 μM) and only partial inhibitor of the channel function, whereas Mg^{2+}, Mn^{2+} and La^{3+} did not exhibit any substantial effect. Co^{2+}, the most potent channel blocker, was able not only to compete with Ca^{2+} but also to pass with it through the open channel of TRPV1. In response to heat activation or vanilloid treatment, Co^{2+} accumulation was verified in TRPV1-transfected cell lines and in the TRPV1+ dorsal root ganglion neurons. The inhibitory effect was also demonstrated in vivo. Co^{2+} applied together with vanilloid agonists attenuated the nocifensive eye wipe response in mice. Different rat TRPV1 pore point mutants (Y627W, N628W, D646N and E651W) were created that can validate the binding site of previously used channel blockers in agonist-evoked $^{45}Ca^{2+}$ influx assays in cells expressing TRPV1. The IC_{50} of Co^{2+} on these point mutants were determined to be reasonably comparable to those on the wild type, which suggests that divalent cations passing through the TRPV1 channel use the same negatively charged amino acids as Ca^{2+}.

Keywords Heavy metals · Somatosensory system · Pain · Calcium channel · TRPV1 · Cobalt

Authors László Pecze and Zoltán Winter contributed equally to this work.

L. Pecze · Z. Winter (✉) · K. Jósvay · C. Kolozsi · T. Letoha · G. Dombi · G. Szakonyi · Z. Oláh
Institute of Pharmaceutical Analysis, Faculty of Pharmacy, University of Szeged, Szeged, Hungary
e-mail: winter.zoltan@brc.mta.hu

L. Pecze · K. Jósvay · F. Ötvös · C. Kolozsi · C. Vizler
Institute of Biochemistry, Biological Research Centre of the Hungarian Academy of Sciences, Szeged, Hungary

D. Budai
Kation Europe, Szeged, Hungary

Z. Oláh
Acheuron Hungary Ltd., Szeged, Hungary

T. Letoha
Pharmacoidea Ltd., Szeged, Hungary

F. Ötvös
Greenformatix Nonprofit Ltd., Szeged, Hungary

Introduction

Small-diameter sensory neurons in the peripheral nervous system (PNS) express the transient receptor potential/vanilloid receptor subtype 1 (TRPV1). Four identical subunits of this protein form a functional Ca^{2+} channel. Similarly to other transient receptor potential channel members, the TRPV1 channel belongs in the large superfamily of cation channels with six transmembrane (TM) segments. Following agonist-induced channel opening, a pore loop between segments TM5 and TM6 serves as a cation filter and entry site [1].

When endovanilloids are produced under various inflammatory conditions around the C and Aδ afferents of these PNS neurons, TRPV1 transmits a specific pain sensation to the brain [2–4]. Besides endovanilloids such as anandamide [5, 6], TRPV1 is activated by acids (pH<6.3) and chemo-irritants such as the exovanilloid capsaicin (CAPS) or resiniferatoxin, a naturally occurring, ultrapotent CAPS analogue with excellent specificity for TRPV1 [2, 7–9]. Moreover, TRPV1 can integrate the effects of heat and vanilloids. The heat-sensing domain has been mapped to the C-terminal intracellular region [3, 9, 10].

The vanilloid binding site is localized between segments TM3 and TM4 of TRPV1 [5]. The pain signal, however, is generated by opening of the Ca^{2+} channel situated between domains TM5 and TM6 of four identical subunits [11, 12]. An acidic peptide motif in the pore loop region of TRPV1 (*D*X*E*XX*E*XX*D*) may serve as a docking site for positively charged ions and channel blockers [13]. However, our sequence comparison and previous in silico model-building efforts have not revealed any obvious homology to other divalent metal ion (M^{2+})-binding structures such as the *EF-hand* (*D*X*D*X*D*GXX*D*XX*E*) or the *Excalibur* (*D*X*D*X*D*XXXC*E*) [13].

Various studies have demonstrated that positively charged molecules can act as TRPV1 receptor channel blockers by plugging the pore. Ruthenium Red (RuRed) (a well-known, but non-specific TRPV1 pore blocker) [11], R_4W_2 (a positively charged hexapeptide) [14] and anti-calmodulins/antipsychotic tricyclics [13] have been shown to be able to bind to the *D*X*E*XX*E*XX*D* domain of TRPV1, whereby they block the movement of Ca^{2+} through the pore region.

We set out to assess the effects of various metal cations at different concentrations on the vanilloid -or heat-induced activity of the TRPV1 channel, focusing on the investigation of the most potent cations in vitro and in vivo. Moreover, in our experiments we aimed to shed light on the characteristics of the gating of the TRPV1 channel in order to improve the understanding of the structure and function of the TRPV1 pore region, which may lead to the development of potentially useful painkiller drugs that modulate the activity of this receptor.

Materials and Methods

Reagents Stock solutions (200 mM) of $CoCl_2$, $NiCl_2$, $ZnSO_4$, $CdCl_2$, $CuSO_4$, $CaCl_2$, $CoCl_2$ and $LaCl_3$ were dissolved in water and diluted as required to the working concentrations. To avoid the precipitation of insoluble $La(OH)_3$ and La $(CO_3)_3$, the formation of radiocolloids and the loss of La^{3+} by adsorption to container surfaces, $LaCl_3$ solution was prepared fresh daily in polyethylene vials [15]. RuRed and capsazepine (CapZ; Sigma-Aldrich, St. Louis, MO) were dissolved in DMSO. CAPS was dissolved initially as a stock solution of 3 mM in 95 % ethanol. The peptide R_4W_2 was synthetized in our laboratories and then dissolved in water and used as a 25 mM stock solution. Amitriptyline (AMI), purchased from Sigma-Aldrich, was dissolved in water.

Plasmids The C-terminally epsilon-tagged rat TRPV1ε plasmid construct was prepared in the metallothionein (pMTH) plasmid vector as described earlier [9]. To avoid cell loss through the Ca^{2+}-excytotoxic mechanism that occurs when TRPV1 is overexpressed at 37 °C, only the basal activity of the pMTH promoter was used. The protein kinase C ε epitope tag allowed immunological detection of the TRPV1ε protein, as earlier described [16]. Mutants Y627W, N628W, D646N and E651W were kindly given by Dr. K. J. Swartz (National Institutes of Health, Bethesda, MD 20892, USA) [17] and subcloned into an EF-promoter-driven green fluorescent protein (EGFP)-tagging plasmid vector. The EGFP tag was used for visual determination of the transfection rate by flow cytofluorometry with a FACS-Calibur instrument (Becton Dickinson, San Jose, CA, USA).

Cell Lines Expressing TRPV1 Ectopically The HaCaT keratinocyte cell line was a kind gift of Prof. B. Farkas (Department of Dermatology, University of Cologne, Federal Republic of Germany) [18]. The COS-7 (CRL-1651) and BALB/c-3T3 (CCL-163) cell lines were obtained from ATCC. The 3T3 and HaCaT cell lines permanently expressing the rat TRPV1 channel were prepared as described earlier [19]. COS7 cells were transiently transfected with plasmid containing the sequence of the Y627W, N628W, D646N or E651W TRPV1 mutants or the wild-type TRPV1 channel, by using the Fugene transfection reagent (Roche, Mannheim, Germany). The transfection efficacy was determined by flow cytofluorometry.

Primary Dorsal Root Ganglion Cultures Were prepared from E16 embryonic rats as reported earlier [9]. Briefly, dorsal root ganglions (DRGs) were dissected and then processed in Hank's balanced salt buffer until plated in Dulbecco's Modified Eagle Medium (DMEM). The DMEM contained 20 mM HEPES, pH 7.4, 7.5 % foetal bovine serum, 7.5 % horse serum, 5 mg/ml uridine supplemented with 2 mg/ml 5-fluoro-2′-deoxyuridine and 40 ng/ml nerve growth factor to inhibit cell division and to promote the differentiation of long neuronal processes, respectively. Cells were seeded on 25 mm glass coverslips.

Cobalt Histochemistry Rat DRG cells attached to the coverslips were washed in buffer A (in millimolars: NaCl, 57.5; KCl, 5; $MgCl_2$, 2; HEPES, 10; glucose, 12; sucrose, 139; pH 7.4) for 2 min, and then incubated at 37 °C for 10 min in Co^{2+}-uptake solution (buffer A+5 mM $CoCl_2$) containing 20 μM CAPS. High (20 μM) capsaicin concentration is used in order to obtain a robust and easily detectable Co^{2+} signal. Following a brief wash in buffer A, the water-soluble Co^{2+} taken up by the cells was precipitated with 0.12 % ammonium polysulphide (Sigma-Aldrich) in buffer A, which resulted in the formation of dark, water-insoluble CoS in TRPV1+ cells. Cells were fixed in 4 % formaldehyde and mounted on glass slides, using Kaiser's glycerol gelatine (Merck, Darmstadt, FRG). Cells were examined under a Nikon light microscope (Melville, NY, USA) and photographed with a SPOT RT-SE™ Digital Camera (Diagnostic Instruments). Pictures of the cells were analysed by means of ImageJ 1.45 s software (National Institutes of Health, USA), and the subsequent statistical analyses were performed with PRISM™ 3.01 software (GraphPad Software, Inc. San Diego, CA, USA).

Vanilloid-Induced $^{45}Ca^{2+}$ Uptake Vanilloid-induced $^{45}Ca^{2+}$ transport was assayed in the HaCaT adherent cell lines ectopically expressing the C-terminally ε-tagged rat TRPV1 (3×10^4 cells/well) and Cos7 cells transiently transfected with rat TRPV1 mutants, seeded in poly-D lysine-coated 96-well plates. Immediately before the transport assay, the cells were washed three times with physiological saline solution at room temperature (20–25 °C). We had previously found that TRPV1-transformed cells functioned in the same manner at room temperature as at 30 °C (data not shown). $^{45}Ca^{2+}$ uptake was performed for 10 min with 0.1 μCi $^{45}Ca^{2+}$ as radioactive tracer in a final volume of 100 μl (1.8 μM). CAPS was diluted from a 3 mM ethanol stock solution to the indicated final concentrations. For the termination of $^{45}Ca^{2+}$ uptake, cells were rapidly washed four additional times with 0.2 ml PBS solution, and then lysed in 80 μl/well RIPA buffer (50 mM Tris–HCl, pH 7.5, 150 mM NaCl, 1 % Triton X-100, 0.5 % deoxycholate, 0.1 % SDS and 5 mM EDTA) for 30 min [8, 9, 20, 21]. Aliquots of the solubilised cell extracts were mixed with 120 μl SuperMiX and counted in a 96-well plate liquid scintillation counter (TopCount-NXT, Packard). To measure the effect of temperature on the TRPV1 function in the $^{45}Ca^{2+}$-uptake assay, TRPV1/HaCaT cells were plated on six-well plates. $^{45}Ca^{2+}$ uptake was evoked with 10 ml preheated buffer. The procedure was followed as described above.

After the measurement, the data were corrected for the basal activity of TRPV1 and normalized from zero to one, where zero denotes the counts per minute in TRPV1/HaCaT cells without CAPS and one denotes the counts per minute in TRPV1/HaCaT cells with CAPS. The results of three parallel measurements were averaged and evaluated with PRISM™ 3.01 software (GraphPad Software, Inc. San Diego, CA, USA). During curve fitting, the “Analyze/Nonlinear regression (curve fit)/Sigmoidal dose–response” menu of PRISM™ software was applied. The curve-fitting equation was: $Y=Y_{\min}+(Y_{\max}-Y_{\min})/(1+10^{(\log EC50-X)})$, where X=logarithm of concentration and Y=the response.

Eye Wipe Tests Eye wipe tests were performed on CD1 mice. A 100 μM CAPS solution, or a solution containing 100 μM CAPS and 1 mM $CoCl_2$, or a solution containing 100 μM CAPS and 5 μM CapZ was dropped into the eye, and the number of defensive wiping movements was then counted.

Statistical Analysis One-way ANOVA followed by Turkey’s post-tests was performed with GraphPad Prism version 3.01 software (GraphPad Software, Inc. San Diego, CA, USA).

Results

In the $^{45}Ca^{2+}$ uptake assay, the EC_{50} of CAPS for wild-type TRPV1 was determined to be 0.0860 μM. Approximately 1 μM CAPS caused the full activation (EC_{100}) of TRPV1 at pH 7.5. Channel blocker-screening assays were therefore carried out with 2 μM CAPS (an excess amount of agonist), which does not cause Ca^{2+} cytotoxicity during the 10-min incubation period. The interactions of the metal ions with TRPV1 were studied by using a vanilloid-induced $^{45}Ca^{2+}$-uptake assay. Experiments were carried out on the TRPV1/HaCaT permanent indicator cell line. Channel opening was induced by CAPS in the presence of progressively increasing M^{2+} concentrations in the uptake solution. Incubation of the cells in uptake solutions containing both $^{45}Ca^{2+}$ and Mg^{2+}, Mn^{2+} or La^{3+} (data not shown) resulted in little or no effect, even at the highest concentration (4 mM), whereas Zn^{2+} proved to be a weak [half-maximal inhibitory concentrations (IC_{50})=27 μM] and only partial inhibitor of the 2 μM CAPS-induced $^{45}Ca^{2+}$ uptake. The other cations effectively blocked the vanilloid-induced Ca^{2+} entry into TRPV1/HaCaT cells, with the following sequence of potency: Co^{2+} (IC_{50}=13 μM)>Cd^{2+} (IC_{50}=38 μM)>Ni^{2+}(IC_{50}=62 μM)>Cu^{2+} (IC_{50}=200 μM; Fig. 1a).

To assess the effect of Co^{2+}, the most potent TRPV1 inhibitor, on the heat-activated TRPV1 channels, the activity of TRPV1 was investigated in the presence either of 2 μM CAPS alone or of 2 μM CAPS+250 μM Co^{2+}, at both 37 and 42 °C. The negative control did not contain CAPS. In this assay, high temperature activated the TRPV1 channels and also increased the CAPS-evoked $^{45}Ca^{2+}$ influx. Co^{2+} reduced both the heat and CAPS-induced $^{45}Ca^{2+}$ influx (Fig. 1b).

To compare the potency of Co^{2+} with those of the other positively charged channel blockers, we measured the IC_{50} values of RuRed, AMI and R_4W_2, which are known to have a docking site in the pore loop of TRPV1. The inhibitor potentials of these pore blockers were measured via the CAPS-induced $^{45}Ca^{2+}$ uptake. All of them inhibited CAPS-activated TRPV1, with the following IC_{50} values: RuRed=1 μM, AMI=20 μM and R_4W_2=100 μM (Fig. 1c).

For a better understanding of the inhibition kinetics of Co^{2+} on TRPV1, increasing concentrations of both Co^{2+} and CAPS were applied in the vanilloid-induced $^{45}Ca^{2+}$-uptake assays. The Ca^{2+} uptake of TRPV1/HaCaT cells was inhibited by the simultaneous presence of Co^{2+} in a dose-dependent manner. However, increasing concentrations of Co^{2+} decreased only the maximal response of efficacy

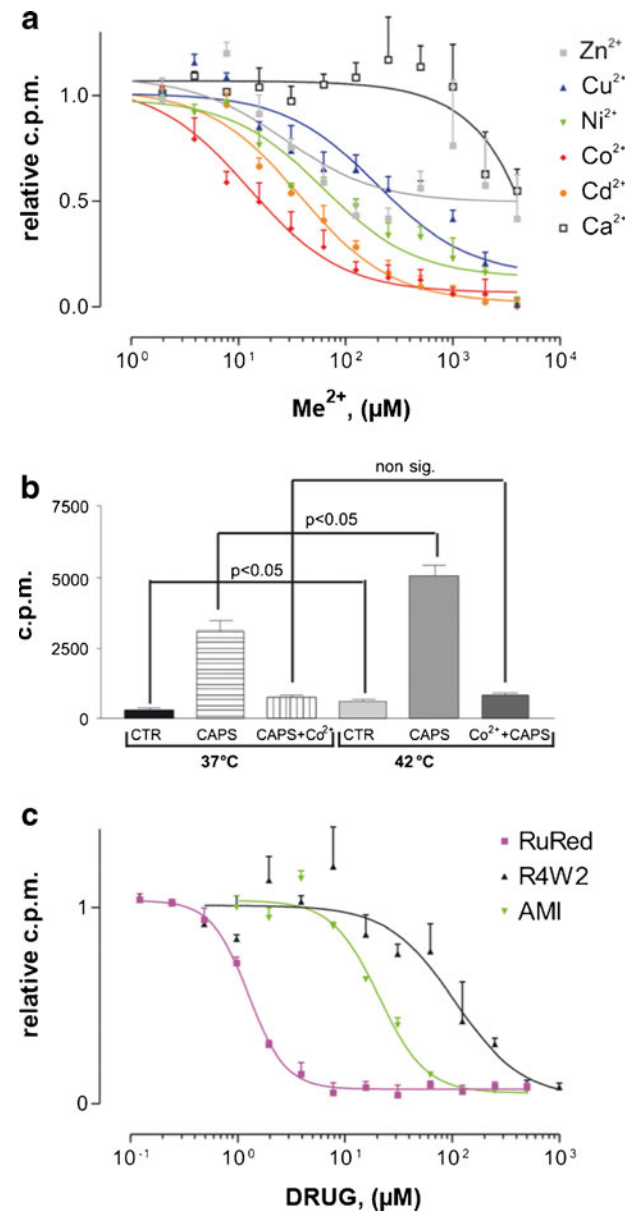

Fig. 1 Ranking divalent cations as channel blockers in cell-based assays. **a** Efficacy of M^{2+} inhibitors of TRPV1 ranked by vanilloid-induced $^{45}Ca^{2+}$ uptake. **b** Co^{2+} inhibits heat-induced Ca^{2+} uptake at 37 °C and at 42 °C. **c** RuRed, R_4W_2 and AMI, previously validated selective channel blockers of TRPV1, were also tested for better comparison of inhibitors. Data are mean values±standard deviation (SD) of the results of three independent experiments. Statistical significance was assessed by post hoc LSD *t* tests after significant one-way analysis of variance (ANOVA). $P<0.05$

(E_{max}) of Ca^{2+} entry; the affinity of CAPS for TRPV1 did not change. The inflection point in the CAPS dose–response curves in each of the Co^{2+} co-incubation studies was found at ~0.08 μM (i.e. EC_{50}), independently of the Co^{2+} concentration. The Co^{2+} inhibition patterns unequivocally indicated channel blocking kinetics (Fig. 2a).

By varying the concentrations of Co^{2+} and Ca^{2+} and measuring the radioactive $^{45}Ca^{2+}$ influx, we assessed whether there was a competition between Co^{2+} and Ca^{2+}. The effect of dilution on the amount of accumulated $^{45}Ca^{2+}$ did not appear at extracellular cold Ca^{2+} concentrations below 1 mM (Fig. 1a), indicating that TRPV1+ cells accumulate Ca^{2+} very effectively from the extracellular space and collect them putatively into ER or mitochondria. Increasing cold Ca^{2+} concentration decreased the inhibitory effect of Co^{2+} (IC_{50} values in the presence of 0, 15.625, 31.25, 62.5 and 125 μM cold Ca^{2+}: 7.944, 51.22, 72.69, 79.09 and 189.1 μM, respectively), showing that the effect of Co^{2+} on Ca^{2+} entry mainly depends on the competition for entry sites. These results suggest that the Co^{2+} entry through the TRPV1 channel is slower, and the Co^{2+} displacing the Ca^{2+} from the pore region of TRPV1 slows down or inhibits the Ca^{2+} uptake (Fig. 2b).

The prolonged agonist stimulation of TRPV1 has been reported to result in an increased permeability to larger cations [22] or small molecules [23], due to conformational changes in the open state of the TRPV1. Thus, we analysed the kinetics of the channel-blocking activity of Co^{2+} by employing different CAPS concentrations. An anticipated shift in the IC_{50} of Co^{2+} would be evidence supporting the idea that Co^{2+} entry depends on the TRPV1 open stages. We indeed observed a shift in the IC_{50} of Co^{2+}, which decreased with increasing CAPS concentration (Fig. 2c). Consequently, increasing agonist concentration enhances the blocking ability of Co^{2+}. To investigate this phenomenon, we plotted the IC_{50} values as a function of CAPS concentration. Curve-fitting analysis confirmed a strong interrelationship between IC_{50} and the CAPS dose applied (Fig. 2d), suggesting that the increased efficiency of inhibition correlates with the different open-state conformations of the TRPV1 channel.

We traced Co^{2+} upon vanilloid induction in sensory neuron cultures prepared from DRGs of rat embryos. To test Co^{2+}-accumulation patterns, cells were co-incubated with 20 μM CAPS in Co^{2+}-containing Ca^{2+}-uptake medium, and the Co^{2+} was then localized by means of NH_4S histochemistry. These experiments revealed that Co^{2+} not only competes with Ca^{2+} but also enters into the cytosol of specific PNS sensory neurons. Functionally responsive vanilloid-sensitive neurons (i.e. $TRPV1^+$) exhibited dark-brown Co^{2+} precipitates inside the rounded neuronal bodies (Fig. 3e). As expected from previous studies, TRPV1 is endogenously expressed in approximately one third of the cultured neurons [24–27]. Without CAPS, no intracellular Co^{2+} accumulation was observed (data not shown). Similar experiments were carried out on rTRPV1/HaCaT and rTRPV1/3T3 cell lines. The accumulation of Co^{2+} was blocked by RuRed, a channel blocker of heat and vanilloid pain signalling. Moreover, the dose-dependent inhibition of the cellular entry of Co^{2+} was determined by the co-application of 5 μM CapZ, a long-known competitive

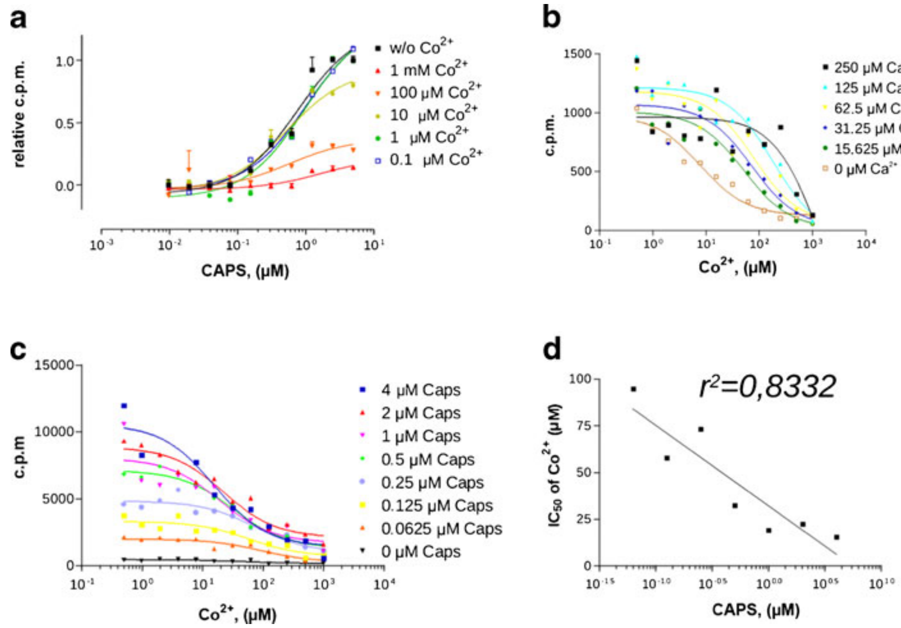

Fig. 2 Co^{2+} inhibits Ca^{2+} entry through the TRPV1 channel. **a** Kinetics of inhibition of Ca^{2+} transport by Co^{2+} in TRPV1+ cells. Data are mean values±SD of the results of three independent experiments. **b** Kinetics of competition between Co^{2+} and cold Ca^{2+} in TRPV1+ cells. **c** Co^{2+} blockage at different CAPS concentrations. Representative data are shown from independent experiments repeated at least three times. **d** IC_{50} values as a function of CAPS concentrations. IC_{50} values of Co^{2+} in the presence of 0.0625, 0.125, 0.25, 0.5, 1, 2 or 4 μM CAPS are 94.81, 57.97, 73.17, 32.6, 19.22, 22.55 and 15.62 μM, respectively

antagonist of pungent vanilloids. After analysis of the photographs of the cells with the ImageJ program, statistical analysis of the data further confirmed our findings: the mean gray values of CAPS-exposed, CAPS-free and CapZ-exposed cells proved to be significantly different (CAPS without Co^{2+}, 72.05±12.38 (S.D.), $n=146$; CAPS+Co^{2+}, 124.4±21.51 (S.D.), $n=111$; CAPS+Co^{2+} + CapZ, 76.92±22.21 (S.D.), $n=100$; P values of the t tests: CAPS without Co^{2+} vs. CAPS+Co^{2+}, $P<0.0001$; CAPS+Co^{2+} vs. CAPS+Co^{2+}+CapZ, $P<0.0001$; CAPS without Co^{2+} vs. CAPS+Co^{2+}+CapZ, $P=0.0290$; Fig. 3). The gray values were measured on the negatives of the images: the darker the cells, the higher the gray values. Analysis of the pictures in Fig. 4, showing TRPV1-expressing HaCaT cells, resulted in the same outcome. Following ANOVA, the groups were compared by using t tests. Each t test except that involving CAPS without Co^{2+} vs. CAPS+Co^{2+}+100 μM CapZ indicated a significant difference between the pairs of groups ($P<0.05$; Fig. 4). No substantial staining could be observed on 3T3 cells (Fig. 5a–e). Statistical analysis of the gray values of the cells indicated no significant darkening in the absence of TRPV1 in the cell membrane.

In order to rule out the possibility that Co^{2+} can enter the cells through VGCCs, 3T3 cells were challenged with 50 mM extracellular KCl. These cells did not show any VGCC activity: the high extracellular KCl concentration-induced depolarization that opens the VGCC channels did not cause $^{45}Ca^{2+}$ accumulation in the $^{45}Ca^{2+}$ -uptake assay.

Moreover, the VGCC blocker nisoldipine did not decrease the CAPS-induced TRPV1-mediated $^{45}Ca^{2+}$ accumulation (data not shown). No Co^{2+} staining was observed in the presence of 50 mM extracellular KCl (Fig. 5f–j). ANOVA indicated no significant differences among the groups ($P=0.9150$). These results confirm that the CAPS-induced Ca^{2+} and Co^{2+} influx in TRPV1/3T3 cells is due exclusively to the TRPV1 channel activity.

Besides the in vitro demonstration of Co^{2+} antagonism, we further validated this Co^{2+} inhibition phenomenon in tests of eye wiping in response to pungent vanilloids [28]. Co^{2+} again decreased the frequency of vanilloid-evoked defending movements. Inhibition experiments with CapZ cross-validated and confirmed our earlier findings (Fig. 6a).

To validate that Co^{2+} inhibition is a consequence of competition with Ca^{2+} for M^{2+}-chelating sites in the pore loop domain, we prepared several point mutants in this region of TRPV1, and determined the channel kinetics through $^{45}Ca^{2+}$-uptake experiments in 3T3 cells expressing the mutant channels. Some of these mutants had been partially characterized earlier in the context of spider venom channel inhibitors [17], and these residues proved to have an important role in the binding of various previously tested channel blockers (RuRed, etc.). Mutated sites are illustrated schematically in Fig. 6b. The EC_{50} and EC_{100} values of mutant channels for CAPS were different from those of the wild type (D646N EC_{50}= 270 nM, E651W EC_{50}=540 nM, N628W EC_{50}=720 nM and Y627W EC_{50}=820 nM), and the blocking effects of Co^{2+} and

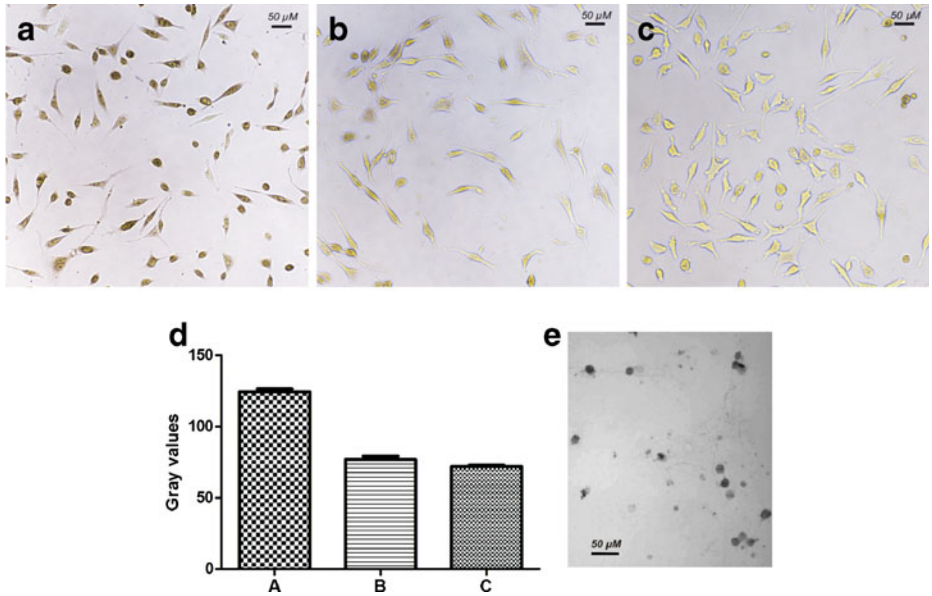

Fig. 3 Co^{2+} histochemistry on the 3T3 cell line expressing TRPV1 ectopically. Cells were incubated for 10 min in buffer A containing **a** 20 μM CAPS+5 mM Co^{2+}; **b** 20 μM CAPS+5 mM Co^{2+}+5 μM CapZ; **c** 5 mM Co^{2+} without CAPS. The dark CoS precipitate indicates the presence of intracellular Co^{2+} that is blockable with CapZ, a competitive antagonist of pungent vanilloids. **d** Gray values of the 3T3 cell line expressing TRPV1 measured by means of ImageJ software. **e** Co^{2+} histochemistry in CAPS-sensitive rat DRG neurons. *Scale bar*=0.05 mm. These results confirm that Co^{2+} not only acts as a blocker but also enters the cell with Ca^{2+} through the TRPV1 channel

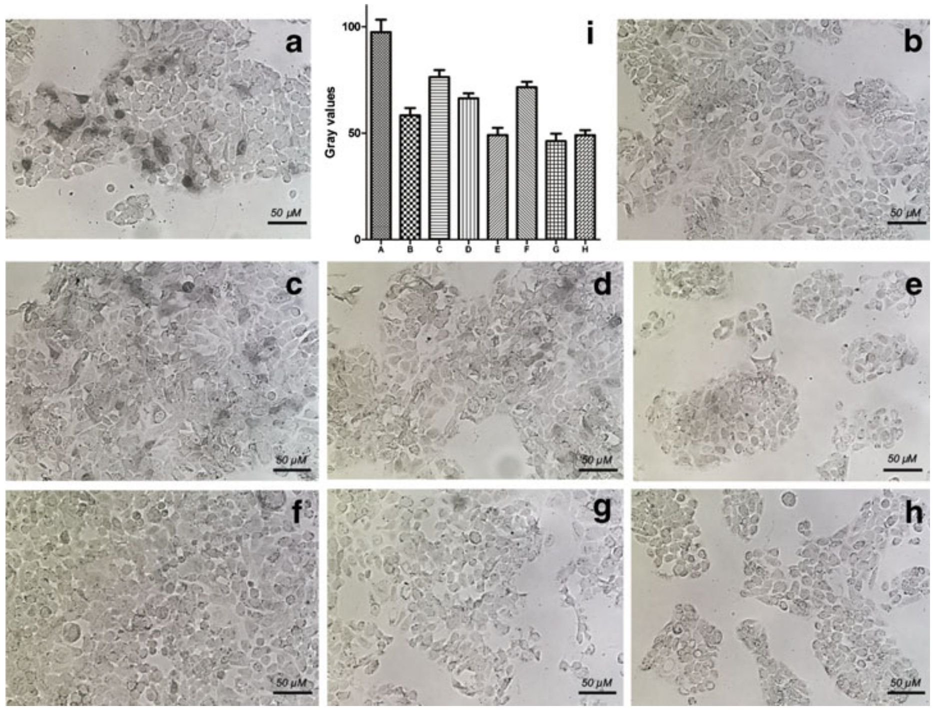

Fig. 4 Co^{2+} histochemistry on the HaCaT cell line expressing TRPV1 ectopically. Cells were incubated for 10 min in buffer A containing **a** 20 μM CAPS+5 mM Co^{2+}; **b** 5 mM Co^{2+} without CAPS; **c** 20 μM CAPS +5 mM Co^{2+}+300 nM CapZ; **d** 20 μM CAPS+5 mM Co^{2+}+5 μM CapZ; **e** 20 μM CAPS+5 mM Co^{2+}+100 μM CapZ; **f** 20 μM CAPS+5 mM Co^{2+}+500 nM RuRed; **g** 20 μM CAPS+5 mM Co^{2+}+7 μM RuRed; **h** 20 μM CAPS+5 mM Co^{2+}+100 μM RuRed. The dark precipitates indicate the presence of intracellular CoS that is blockable with RuRed, a channel blocker of heat and vanilloid pain signalling. Co-application of CapZ, a competitive antagonist of pungent vanilloids, also inhibited the cellular entry of Co^{2+} in a dose-dependent manner: this is a well-characterized evidence-based method of localization of intracellular Co^{2+}. *I*: Gray values of the HaCaT cell line expressing TRPV1 measured by means of ImageJ software

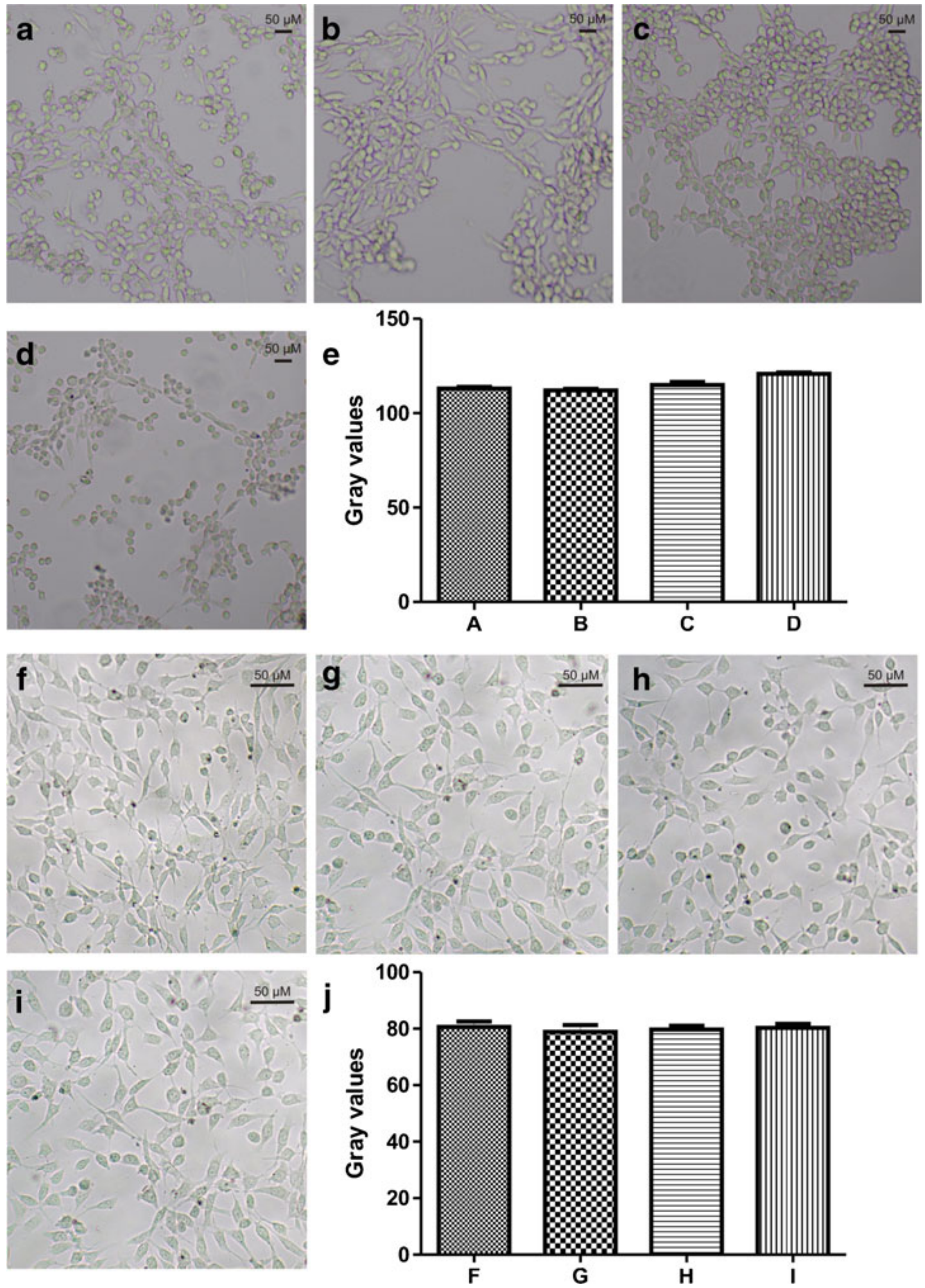

Fig. 5 Co^{2+} histochemistry on the 3 T3 cell line. Cells were incubated for 10 min in buffer A containing: **a** 20 μM CAPS+5 mM Co^{2+}; **b** 20 μM CAPS+5 mM Co^{2+}+5 μM CapZ; **c** 5 mM Co^{2+} without CAPS. **d** 20 μM CAPS without Co^{2+}. No CoS precipitate could be observed in the absence of TRPV1 protein in the cell membrane. **e** Gray values of the 3T3 cell line measured by means of ImageJ software. Cells were incubated for 10 min in: **f** buffer A containing 5 mM Co^{2+}; **g** buffer A without Co^{2+}; **h** modified buffer A containing 50 mM KCl+2.5 mM NaCl+5 mM Co^{2+}; **i** modified buffer A containing 50 mM KCl+12.5 mM NaCl without Co^{2+}. **j** Gray values of the 3T3 cell line measured by means of ImageJ software. These results confirm that Co^{2+} does not enter the 3T3 cells through VGCCs

RuRed on TRPV1 mutants were therefore analysed with 4 μM CAPS. The neutralization of D646 reduced the sensitivity of TRPV1 to RuRed inhibition [11]. Our $^{45}Ca^{2+}$-influx studies on TRPV1 point mutants revealed the following IC_{50} data for RuRed: IC_{50} (D646N)=12.8 μM>IC_{50} (N628W)= 1.33 μM>IC_{50} (E651W)=0.94 μM>IC_{50} (wild type)= 0.87 μM>IC_{50} (Y627W)=0.26 μM (Fig. 6c), which findings correspond with published results [17]. Likewise, Co^{2+} inhibited the 4 μM CAPS-evoked $^{45}Ca^{2+}$ influx in the D646N and E651W point mutants similarly as determined in the wild type. The neutralization of D646 caused no or only a minimal change in IC_{50}. As compared with the wild type in this representative experiment, Co^{2+} sensitivity was slightly reduced in the D646N mutant (IC_{50}=18.3 vs. 25.7 μM). The Y627W, N628W and E651W mutants displayed little or no difference relative to the wild type (IC_{50}=18.6, 16.4 and 15.3 μM, respectively vs. 18.3 μM; Fig. 6d). Based on these findings, inhibition seems to be a consequence of competition with Ca^{2+} for M^{2+}-chelating sites in the pore loop domain.

Discussion

Testing the effects of various metal cations on the vanilloid-induced activity of the TRPV1 channel, we demonstrated that Mg^{2+}, Mn^{2+} or La^{3+} caused little or no decrease in

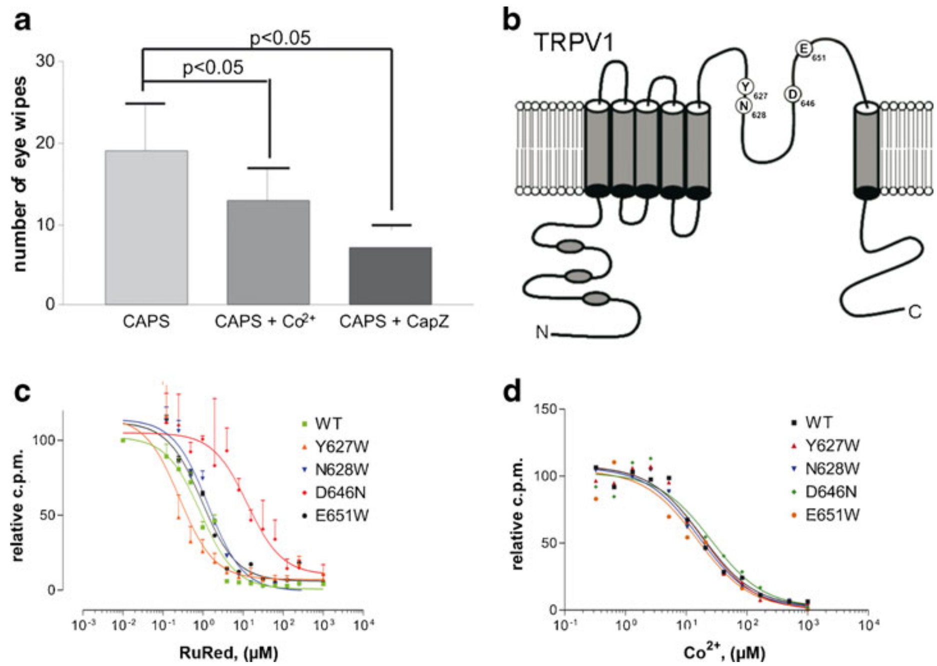

Fig. 6 Eye wipe test performed on CD1 mice and cobalt uptake experiments on TRPV1 point mutants. **a** Eye wipe responses to the corneal application of CAPS alone or together with Co^{2+} or CapZ. Statistical significance of inhibition was assessed by means of the paired *t* test ($P<0.05$). Data are means±SD of the results of eight independent experiments ($n=8$). **b** Schematic localizations of the mutants used in the study. **c**, **d** IC_{50} of RuRed and Co^{2+} determined on TRPV1 point mutants and wild type (WT). Data are means±SD of the results of three independent experiments. TRPV1 point mutants revealed that the binding regions of Co^{2+} and RuRed are different

channel activity, whereas Zn^{2+} proved to be a weak and only partial inhibitor of the 2 μM CAPS-induced $^{45}Ca^{2+}$ uptake. The other cations effectively blocked the vanilloid-induced Ca^{2+} entry into TRPV1/HaCaT cells, with the following sequence of potency: $Co^{2+}>Cd^{2+}>Ni^{2+}>Cu^{2+}$.

It was reported by Nilius et al. [29] that Co^{2+} reduced the inward Ca^{2+} current through ECaC1 (TRPV5), a close relative of TRPV1, sharing around 30 % homology with it. Fast and reversible recovery of the current upon washout of the inhibitor was detected during their experiments. Furthermore, they identified other M^{2+}-s as effective inhibitors of the Ca^{2+} influx. Their results indicated the following overall blocking sequence: $Pb^{2+}=Cu^{2+}=Gd^{3+}>Cd^{2+}>Zn^{2+}>La^{3+}>Co^{2+}>Fe^{2+}>>Fe^{3+}$. Zeng et al. found Cu^{2+} to be a potent inhibitor of the whole-cell current evoked by intracellular ADP-ribose through TRPM2, another member of the TRP group. The inhibitory effect of Cu^{2+} was irreversible, and occurred only if Cu^{2+} was administered in outside-out patches, suggesting that the action site is located extracellularly. The TRPM2 current was also blocked by Hg^{2+}, Pb^{2+}, Fe^{2+} and Se^{2+} [30].

In accord with the above-mentioned findings, we also observed ion influx-inhibitory effects of M^{2+}-s on TRP channel. Depending on the TRP channel type, differences of the orders of blocking potency could be detected. Furthermore, the blocking effects of the individual cations could be reversible or irreversible, depending on the channel type. The three channels are close relatives and share high degree of sequence and structural homology with one another, which explains the similar responses to M^{2+}-s. Having diverged from a common ancestor, TRP channels operate on uniform principles. However, during evolution TRP superfamily has evolved for various specialized functions. TRPV1 and TRPV5, for example, belong to different subgroups of the TRPV family; TRPV1–4 are non-ion-selective, whilst TRPV5–6 are highly Ca^{2+}-selective. Hence, this functional adaptation may cause the differences in the M^{2+}-evoked responses.

As concerns our own results, Co^{2+} reduced not only CAPS-induced but also heat-induced $^{45}Ca^{2+}$ influx. When increasing concentrations of both Co^{2+} and CAPS were applied, the Co^{2+} inhibition patterns indicated channel-blocking kinetics. Our dose–response and Co^{2+} accumulation experiments revealed a competition for binding sites and a co-entry mechanism. We presume that Co^{2+} inhibits TRPV1 through its ability to bind to the ion selectivity filter of the channel: it passes through the ion channel much more slowly than Ca^{2+}. Ca^{2+} entry is also slowed down by the binding of Co^{2+}, which occupies the appropriate amino acid residues of the ion selectivity filter. This hypothesis seems to be further supported by the findings of Sajadi [31], who determined the stability constants of the 1:1 complexes formed between M^{2+} and L-tryptophan and other amino acids. The sequence obtained in the case of tryptophan was $Ca^{2+}<Mg^{2+}<Mn^{2+}<Co^{2+}<Ni^{2+}<Cu^{2+}>Zn^{2+}$, which follows the Irving-Williams sequence [32]. The order of the stability constants was similar in the cases of methionine, alanine, leucine, valine and glycine. The amino acid sequence of the putative pore region is STSHRWRGPACRPPDSSYNSLYSTCLELFKFTIGMGD (Q8NER1, UniProt), containing all the tested amino acids but valine. The stability constants formed between M^{2+} and tryptophan were Ca^{2+}, 2.55±0.08; Mg^{2+}, 2.84±0.08; Mn^{2+}, 3.34±0.05; Co^{2+}, 4.34±0.07; Ni^{2+}, 5.31±0.06; Cu^{2+}, 8.05±0.05 and Zn^{2+}, 5.00±0.08. The stability constants for Mg^{2+} and Mn^{2+} are close to that of Ca^{2+}, so these ions can probably readily pass through the open channel of TRPV1. Co^{2+}, Ni^{2+} and Cu^{2+} can be characterized by much higher complex-forming strength, elucidating the elevated TRPV1 blocking potency. Interestingly, for these three M^{2+}-s, an unexpected relationship can be observed between the stability constant and the TRPV1 blocking potency. The stronger the bond, the weaker the TRPV1 inhibition potency is. The ionic radii (in picometres) of these cations are Ca^{2+}, 100; Mg^{2+}, 72; Mn^{2+}, 67; Co^{2+}, 65; Ni^{2+}, 69; Cu^{2+}, 73 and Zn^{2+}, 74 [33]. Ca^{2+} is likely to have the ideal ionic radius and stability constant in its reactions with amino acids in order to be effectively passed along the carbonyl groups of the peptide backbone in the ion selectivity filter and the pore loop. Co^{2+} has a medium stability constant and the smallest ionic radius, which is probably not adequate for efficient transport. These two parameters seem to be equally involved in the proper ion influx. The stronger the M^{2+}-amino acid complex and the smaller the ionic radius is, the more probable it is that M^{2+} will block the Ca^{2+} influx through the TRPV1 channel. As another interesting finding, in our experiments, Zn^{2+}seemed to be only weak and partial inhibitor of the ion current. Its stability constant is almost as high as that of Co^{2+}, suggesting a strong TRPV1-blocking ability, whereas its ionic radius is much larger than that of Co^{2+}. Interestingly, the IC_{50} of Zn^{2+} is the second lowest exceeding only that of Co^{2+}, but Zn^{2+} can achieve a decrease of merely 30 % of the maximal ion influx.

The TRPV1 channel is a non-selective cation channel, and still shows preference for Ca^{2+}. The sequence of permeability is $Ca^{2+}>Mg^{2+}>Na^{+}=K^{+}=Cs^{+}$ [3]. In addition to all these, TRPV1 also conducts protons [34]. Following prolonged exposure to agonists, TRPV1 becomes permeable even to larger organic cations, including dyes such as YO-PRO1 and FM1-43 [22] and a lidocaine derivative QX-314 [23]. Increasing agonist concentration enhances the blocking ability of Co^{2+}, suggesting a correlation between the increased efficacy of inhibition and the different open-state conformations of the TRPV1 channel. Further experiments (involving patch-clamp recordings) would be needed to clarify the inhibitory effect of Co^{2+} on the fluxes of the other cations or molecules mentioned above. However, no channel blocker or antagonist of TRPV1 has been reported that is able to block the flux of only one specific ion, and antagonists seem to block all these influxes. For example, CapZ blocks the influxes of both Ca^{2+} and Na^{+} [35]. Overall, we presume that Co^{2+} can also block the ion currents mentioned above.

Before the exploration of TRPV1 protein, Co^{2+} histochemistry was a very useful tool for the identification of vanilloid-sensitive primary afferent neurons with C-and Aδ fibres after in vivo experiments. Co^{2+} uptake and the post-mortem determination of Co^{2+} deposits quite accurately identified C-and Aδ afferents, the neuronal subset that can be activated by treatment with a vanilloid agonist, CAPS [36, 37]. Likewise, as previously documented in a subpopulation of pseudo-unipolar neurons [38], we have now demonstrated selective vanilloid-induced Co^{2+} accumulation in the cytosol of DRG primary cultures and TRPV1-transfected HaCaT and 3T3 cells. The accumulation of Co^{2+} could be blocked by RuRed or CapZ in a dose-dependent manner. The CAPS-induced Ca^{2+} and Co^{2+} influxes in TRPV1/3T3 cells proved to be due exclusively to the TRPV1 channel and not to VGCC activity.

Co^{2+} inhibited the pain-evoked defensive movements in eye wipe tests in response to pungent vanilloids. However, not only TRPV1 but also some other calcium channels of the sensory neurons, such as VGCCs, can be blocked by Co^{2+} [39]. VGCCs share structural homology with TRPV1 channel. The α1 subunit of voltage-gated calcium channels is organized in four homologous domains (I–IV), with six transmembrane segments (S1–S6) in each [40]. There is an additional region (H5) between S5 and S6, which forms a part of the pore region of the channel [41]. Within each H5 region, there exist conserved glutamate residues, significantly homologous to conventional EF-hand motifs [42], acting as the selectivity filter [43]. Mn^{2+}, Ni^{2+} and Cd^{2+} in contrast with Co^{2+} are known to be stronger blockers of the VGCCs. Cu^{2+}, Mn^{2+} and Co^{2+} blocked high-voltage activated currents conducted by Ba^{2+} with IC_{50} of 920, 58, and 65 μM, respectively [44, 45]. All of these ions exert their effects through high-affinity docking to the cation-binding site at the IIIS5–H5 pore region of the VACCs [46, 47]. Since Co^{2+} has higher IC_{50} for VGCCs (≈65 μM) than for TRPV1 (≈15 μM), we can conclude that decrease in the number of eye wipes might be due, at least partially, to an inhibitory effect of Co^{2+} on TRPV1.

Positively charged tricyclics, K/R-rich basic peptides and RuRed dock to the DXEXXEXXD motif at the channel orifice [13]. Although our point mutants overlap with the RuRed docking site [11, 14, 45], our point mutant studies suggest that Co^{2+} has a different binding site. Accordingly, the D646N point mutant, which is crucial for RuRed binding, does not change the kinetic parameters of Co^{2+} inhibition in cells ectopically expressing the D646N mutant TRPV1. We carried out vanilloid-induced $^{45}Ca^{2+}$-uptake experiments with channel point mutants of TRPV1 in which the agonist binding site remained intact. Interestingly, no significantly decreased efficacy of Co^{2+} inhibition was found when ^{646}aspartate was replaced by asparagine. Based on these results, Co^{2+} is supposed to evoke its effect at a different site on the pore loop region than RuRed, or to use the same negatively charged amino acids passing through the TRPV1 channel as Ca^{2+}. This line of research on functional point mutants should be continued to determine whether Co^{2+} has a specific binding site on the channel orifice or not.

Most painkiller drugs are competitive agonists and target the CAPS-binding domain [48]. As the 646***D***L***E***FT***E***NY***D*** acidic tetrad sequence of the TRPV1 receptor is unique among Ca^{2+}-binding proteins, this permits the design of painkillers targeting the channel orifice of TRPV1 and acting as channel blockers. A better understanding of the structural background and dynamics of the competition of Ca^{2+} with other M^{2+} for entry may result in the discovery of novel channel blocker painkillers. Furthermore, our data can contribute to a better understanding of the structures and functions of all TRP superfamily members. The specific effect of the selected M^{2+}-s on the given ion channel pore region can serve as a valuable constraint during in silico modelling of the pore region. By comparing the different cation action profiles of pore regions, the model can be fine-tuned. The mechanism of Co^{2+}-mediated inhibition provides screening for adjuvant therapeutics with higher selectivity than that of AMI, an approved drug currently used in clinical practice, but with only limited efficacy and with serious side effects.

Acknowledgments The excellent technical assistance of Erzsébet Kusz in the preparation of the cell lines is acknowledged. This work was supported by grants from the National Office for Research and Technology (OMFB-01630; OMFB-01703, OMFB-01576/2006 and BAROSS_DA07-DA_TECH_07-2008-0043). TL was supported by a Postdoctoral Fellowship of the Zoltán Magyary Foundation. ZO was supported by Marie Curie European Re-integration Grant MC-IRG030854-PAINKILLER; Ányos Jedlik Program NKFP-1-00019/2005; GVOP-3.3.1-05/1.-2005-05-0057/3.0, and BAROSS_DA07-DA_TECH_07-2008-0028. CV was supported by grants from the National Office for Research and Technology (OM-00051/2005, OMFB-01575/2006, ERC_HU_09 3D_TRPV1 OMFB-01813/2009 and TÁMOP-4.2.1.B-09/1/KONV) and the Hungarian Ministry of Health (552/2006). GS and CV are grateful for the award of Bolyai Fellowships of the Hungarian Academy of Sciences. The authors would like to express their appreciation to our native speaker lector for proofreading the manuscript.

References

1. Latorre R (2009) Perspectives on TRP channel structure and the TRPA1 puzzle. J Gen Physiol 133(3):227–229
2. Tender GC, Walbridge S, Olah Z, Karai L, Iadarola M, Oldfield EH, Lonser RR (2005) Selective ablation of nociceptive neurons for elimination of hyperalgesia and neurogenic inflammation. J Neurosurg 102(3):522–525
3. Caterina MJ, Schumacher MA, Tominaga M, Rosen TA, Levine JD, Julius D (1997) The capsaicin receptor: a heat-activated ion channel in the pain pathway. Nature 389(6653):816–824. doi:10.1038/39807
4. Naziroglu M, Dikici DM, Dursun S (2012) Role of oxidative stress and Ca (2)(+) signaling on molecular pathways of neuropathic pain in diabetes: focus on TRP channels. Neurochem Res 37(10):2065–2075. doi:10.1007/s11064-012-0850-x
5. Gavva NR, Klionsky L, Qu Y, Shi L, Tamir R, Edenson S, Zhang TJ, Viswanadhan VN, Toth A, Pearce LV, Vanderah TW, Porreca F, Blumberg PM, Lile J, Sun Y, Wild K, Louis JC, Treanor JJ (2004) Molecular determinants of vanilloid sensitivity in TRPV1. J Biol Chem 279(19):20283–20295. doi:10.1074/jbc.M312577200M312577200
6. Olah Z, Karai L, Iadarola MJ (2002) Protein kinase C(alpha) is required for vanilloid receptor 1 activation. Evidence for multiple signaling pathways. J Biol Chem 277(38):35752–35759
7. Brown DC, Iadarola MJ, Perkowski SZ, Erin H, Shofer F, Laszlo KJ, Olah Z, Mannes AJ (2005) Physiologic and antinociceptive effects of intrathecal resiniferatoxin in a canine bone cancer model. Anesthesiology 103(5):1052–1059
8. Karai L, Brown DC, Mannes AJ, Connelly ST, Brown J, Gandal M, Wellisch OM, Neubert JK, Olah Z, Iadarola MJ (2004) Deletion of vanilloid receptor 1-expressing primary afferent neurons for pain control. J Clin Invest 113(9):1344–1352
9. Kedei N, Szabo T, Lile JD, Treanor JJ, Olah Z, Iadarola MJ, Blumberg PM (2001) Analysis of the native quaternary structure of vanilloid receptor 1. J Biol Chem 276(30):28613–28619. doi:10.1074/jbc.M103272200M103272200
10. Tominaga M, Caterina MJ, Malmberg AB, Rosen TA, Gilbert H, Skinner K, Raumann BE, Basbaum AI, Julius D (1998) The cloned capsaicin receptor integrates multiple pain-producing stimuli. Neuron 21(3):531–543
11. Garcia-Martinez C, Morenilla-Palao C, Planells-Cases R, Merino JM, Ferrer-Montiel A (2000) Identification of an aspartic residue in the P-loop of the vanilloid receptor that modulates pore properties. J Biol Chem 275(42):32552–32558. doi:10.1074/jbc.M002391200M002391200
12. Jara-Oseguera AN-PA, Szallasi A, Islas L, Rosenbaum T (2010) Molecular mechanisms of TRPV1 channel activation. Open Pain J 3:68–81
13. Olah Z, Josvay K, Pecze L, Letoha T, Babai N, Budai D, Otvos F, Szalma S, Vizler C (2007) Anti-calmodulins and tricyclic adjuvants in pain therapy block the TRPV1 channel. PLoS One 2(6):e545
14. Himmel HM, Kiss T, Borvendeg SJ, Gillen C, Illes P (2002) The arginine-rich hexapeptide R4W2 is a stereoselective antagonist at the vanilloid receptor 1: a Ca2+ imaging study in adult rat dorsal root ganglion neurons. J Pharmacol Exp Ther 301(3):981–986
15. Enyeart JJ, Xu L, Enyeart JA (2002) Dual actions of lanthanides on ACTH-inhibited leak K(+) channels. Am J Physiol Endocrinol Metab 282(6):E1255–1266
16. Olah Z, Lehel C, Jakab G, Anderson WB (1994) A cloning and epsilon-epitope-tagging insert for the expression of polymerase chain reaction-generated cDNA fragments in *Escherichia coli* and mammalian cells. Anal Biochem 221(1):94–102
17. Kitaguchi T, Swartz KJ (2005) An inhibitor of TRPV1 channels isolated from funnel Web spider venom. Biochemistry 44 (47):15544–15549
18. Farkas B, Bonnekoh B, Mahrle G (1991) Repeated treatment with dithranol induces a tolerance reaction in keratinocytes in vitro. Arch Dermatol Res 283(5):337–341
19. Pecze L, Szabo K, Szell M, Josvay K, Kaszas K, Kusz E, Letoha T, Prorok J, Koncz I, Toth A, Kemeny L, Vizler C, Olah Z (2008) Human keratinocytes are vanilloid resistant. PLoS One 3(10):e3419
20. Clapham DE, Montell C, Schultz G, Julius D (2003) International Union of Pharmacology. XLIII. Compendium of voltage-gated ion channels: transient receptor potential channels. Pharmacol Rev 55 (4):591–596. doi:10.1124/pr.55.4.655/4/591
21. Marshall IC, Owen DE, Cripps TV, Davis JB, McNulty S, Smart D (2003) Activation of vanilloid receptor 1 by resiniferatoxin

mobilizes calcium from inositol 1, 4, 5-trisphosphate-sensitive stores. Br J Pharmacol 138(1):172–176
22. Chung MK, Guler AD, Caterina MJ (2008) TRPV1 shows dynamic ionic selectivity during agonist stimulation. Nat Neurosci 11 (5):555–564
23. Binshtok AM, Bean BP, Woolf CJ (2007) Inhibition of nociceptors by TRPV1-mediated entry of impermeant sodium channel blockers. Nature 449(7162):607–610. doi:10.1038/nature06191
24. Fernihough J, Gentry C, Bevan S, Winter J (2005) Regulation of calcitonin gene-related peptide and TRPV1 in a rat model of osteoarthritis. Neurosci Lett 388(2):75–80. doi:10.1016/j.neulet.2005.06.044
25. Ji RR, Samad TA, Jin SX, Schmoll R, Woolf CJ (2002) p38 MAPK activation by NGF in primary sensory neurons after inflammation increases TRPV1 levels and maintains heat hyperalgesia. Neuron 36(1):57–68
26. Malin S, Molliver D, Christianson JA, Schwartz ES, Cornuet P, Albers KM, Davis BM (2011) TRPV1 and TRPA1 function and modulation are target tissue dependent. J Neurosci 31(29):10516–10528. doi:10.1523/JNEUROSCI.2992-10.2011
27. Zhang X, Huang J, McNaughton PA (2005) NGF rapidly increases membrane expression of TRPV1 heat-gated ion channels. Embo J 24(24):4211–4223. doi:10.1038/sj.emboj.7600893
28. Pecze L, Pelsoczi P, Kecskes M, Winter Z, Papp A, Kaszas K, Letoha T, Vizler C, Olah Z (2009) Resiniferatoxin mediated ablation of TRPV1+ neurons removes TRPA1 as well. Can J Neurol Sci 36(2):234–241
29. Nilius B, Prenen J, Vennekens R, Hoenderop JG, Bindels RJ, Droogmans G (2001) Pharmacological modulation of monovalent cation currents through the epithelial Ca2+ channel ECaC1. Br J Pharmacol 134(3):453–462. doi:10.1038/sj.bjp.0704272
30. Zeng B, Chen GL, Xu SZ (2012) Divalent copper is a potent extracellular blocker for TRPM2 channel. Biochem Biophys Res Commun 424(2):279–284. doi:10.1016/j.bbrc.2012.06.107
31. Sajadi SAA (2011) Complex bilding behavior of L-tryptophan and related amino acids, a comparative investigation. Am J Chem 1 (2):60–64. doi:10.5923/j.chemistry.20110102.13
32. Irving H, Williams RJP (1953) The stability of transition-metal complexes. J Chem Soc (637):3192–3210. doi:10.1039/JR9530003192
33. Shannon R (1976) Revised effective ionic radii and systematic studies of interatomic distances in halides and chalcogenides. Acta Crystallogr A 32(5):751–767. doi:10.1107/S0567739476001551
34. Vulcu SD, Liewald JF, Gillen C, Rupp J, Nawrath H (2004) Proton conductance of human transient receptor potential-vanilloid type-1 expressed in oocytes of *Xenopus laevis* and in Chinese hamster ovary cells. Neuroscience 125(4):861–866. doi:10.1016/j.neuroscience.2004.02.032
35. Grant ER, Dubin AE, Zhang SP, Zivin RA, Zhong Z (2002) Simultaneous intracellular calcium and sodium flux imaging in human vanilloid receptor 1 (VR1)-transfected human embryonic kidney cells: a method to resolve ionic dependence of VR1-mediated cell death. J Pharmacol Exp Ther 300(1):9–17
36. Hu-Tsai M, Winter J, Woolf CJ (1992) Regional differences in the distribution of capsaicin-sensitive target-identified adult rat dorsal root ganglion neurons. Neurosci Lett 143(1–2):251–254
37. Winter J, Evison CJ, O'Brien C, Benowitz L, Lindsay RM, Mulderry P, Woolf C (1992) Neurotoxic damage evokes regenerative responses from adult rat sensory neurones. Neurosci Lett 146(1):48–52
38. Reichling DB, Barratt L, Levine JD (1997) Heat-induced cobalt entry: an assay for heat transduction in cultured rat dorsal root ganglion neurons. Neuroscience 77(2):291–294
39. Nishimura T, Krier J, Akasu T (1993) Effects of vasoactive intestinal contractor on voltage-activated Ca2+ currents in feline parasympathetic neurons. Am J Physiol 265(6.1):1158–1168
40. Catterall WA, Perez-Reyes E, Snutch TP, Striessnig J (2005) International Union of Pharmacology. XLVIII. Nomenclature and structure–function relationships of voltage-gated calcium channels. Pharmacol Rev 57(4):411–425. doi:10.1124/pr.57.4.5
41. Guy HR, Conti F (1990) Pursuing the structure and function of voltage-gated channels. Trends Neurosci 13(6):201–206
42. Doughty SW, Blaney FE, Orlek BS, Richards WG (1998) A molecular mechanism for toxin block in N-type calcium channels. Protein Eng 11(2):95–99
43. Mikala G, Bahinski A, Yatani A, Tang S, Schwartz A (1993) Differential contribution by conserved glutamate residues to an ion-selectivity site in the L-type Ca2+ channel pore. Febs Lett 335(2):265–269
44. Castelli L, Tanzi F, Taglietti V, Magistretti J (2003) Cu2+, Co2+, and Mn2+ modify the gating kinetics of high-voltage-activated Ca2+ channels in rat palaeocortical neurons. J Membr Biol 195 (3):121–136
45. Hagiwara S, Byerly L (1981) Calcium channel. Annu Rev Neurosci 4:69–125
46. Thevenod F, Jones SW (1992) Cadmium block of calcium current in frog sympathetic neurons. Biophys J 63(1):162–168
47. Winegar BD, Kelly R, Lansman JB (1991) Block of current through single calcium channels by Fe, Co, and Ni. Location of the transition metal binding site in the pore. J Gen Physiol 97 (2):351–367
48. Gavva NR, Tamir R, Klionsky L, Norman MH, Louis JC, Wild KD, Treanor JJ (2005) Proton activation does not alter antagonist interaction with the capsaicin-binding pocket of TRPV1. Mol Pharmacol 68(6):1524–1533